# Considerations for MESF-bead based assignment of absolute fluorescence values to nanoparticles and extracellular vesicles by flow cytometry

**Estefanía Lozano-Andrés[1, #], Tina Van Den Broeck[2, #], Lili Wang[3], Majid Mehrpouyan[4], Ye Tian[5], Xiaomei Yan[5], Marca H.M. Wauben*[1, #], Ger J.A. Arkesteijn*[1]**

1 Department of Biomolecular Health Sciences, Faculty of Veterinary Medicine, Utrecht University, Utrecht, The Netherlands

2 BD Biosciences, Erembodegem, Belgium

3 Biosystems and Biomaterials Division, National Institutes of Standards and Technology (NIST), Gaithersburg, MD 20899, USA

4 BD Biosciences, San Jose, CA 95131, USA

5 Department of Chemical Biology, MOE Key Laboratory of Spectrochemical Analysis & Instrumentation, Key Laboratory for Chemical Biology of Fujian Province, College of Chemistry and Chemical Engineering, Xiamen University, Xiamen 361005, People's Republic of China

# TRAIN-EV Marie Skłodowska-Curie Action-Innovative Training Network, train-ev.eu

*Both authors contributed equally

**Corresponding author:**

Dr. G.J.A. Arkesteijn

Department of Biomolecular Health Sciences

Faculty of Veterinary Sciences

Utrecht University

Yalelaan 2, 3584 CM

Utrecht, The Netherlands

T: +31 30 2535451/2535833

E: G.J.A.Arkesteijn@uu.nl

**Abstract**

Flow cytometry is a promising technique to characterize nanoparticles (NPs) and extracellular vesicles (EVs). However, the majority of reported experiments, use arbitrary units to indicate fluorescence intensity. This hampers comparison of results from different laboratories and different platforms. We investigated the advised use of calibrated molecules of equivalent soluble fluorophores (MESF)-beads for assignment of absolute fluorescence to NPs and EVs. Firstly, we evaluated the use of two different FITC MESF bead sets as calibrators on three different flow cytometry platforms (BD Influx™, CytoFLEX LX™ and SORP BD FACSCelesta™). Secondly, NPs and biological 4T1 mammary carcinoma-EVs were analyzed using the BD Influx and their fluorescence signals calibrated by using different sets of FITC and PE MESF beads. Although fluorescence calibration, using bright calibrators designed for cellular flow cytometry, makes inter-platform comparison possible for fluorescently labeled cells and brightly labeled particles, but the uncertainty of the currently available calibrators, which are far out of the fluorescence range of the sub-micron particles, hampers a reliable assignment of absolute MESF numbers based on

extrapolation into the dim fluorescence range. Our results illustrate the need for calibration materials specifically designed for NPs and EVs to enable a reliable assignment of absolute fluorescence values in the lower fluorescent ranges.

**Key words:** flow cytometry, fluorescence calibration, standardization, MESF, extracellular vesicles, nanoparticles

## Introduction

Flow cytometry has attracted the attention of many researchers working in the field of cell-derived extracellular vesicles (EVs) as a valuable tool for high-throughput single particle-based analysis [1]. It allows for quantitative multiparametric characterization of subsets of EVs within the heterogeneous EV-population based on the detection of light scatter signals and fluorescence. Although flow cytometry is one of the methods of choice for EV analysis, several requirements need to be met and data need to be reported in a proper way to improve rigor and reproducibility of flow cytometric EV analysis [2]. In spite of the advancements made in the past years, the vast majority of EV flow cytometric data is still published in arbitrary units. While expressing percentages of subpopulations or median fluorescence intensity (MFI) relative to the experimental controls is a common practice for cell measurements by flow cytometry, this approach is less desirable for the reliable analysis of the much smaller and dimmer EVs whereby positively-stained events cannot be discriminated from negative counterparts as a clearly separate population. Especially for these small and dim particles, the variability between the measured outcome caused by the diversity in fluidics, optics and electronics between different platforms inevitably will be reflected in the results reported as arbitrary units of fluorescence. Calibration could make clear whether a specific instrument can fully resolve or partly detect a certain EV or NP population.

71 Altogether, the use of standardized units for EV flow cytometric analysis will strongly contribute
72 to rigor and reproducibility and makes inter-platform and inter-laboratory analysis possible.
73 Therefore, the three-society EV flow cytometry working group, i.e. ISEV-ISAC-ISTH EV flow
74 workgroup, has recommended in the recently published MIFlowCyt-EV framework for
75 standardized reporting of EV flow cytometry experiments, the use of fluorescence calibration [2].
76 Fluorescence calibration is successfully applied for cell flow cytometry in which arbitrary units are
77 translated to standardized units of fluorescence that are established by National Institute of
78 Standards and Technology (NIST), such as molecules of equivalent soluble fluorophores (MESF)
79 or equivalent number of reference fluorophore (ERF) [3-6]. The currently available calibrator
80 materials are designed for the calibration of fluorescence of labeled cells and hence are much
81 brighter in fluorescence when compared to the fluorescence from stained EVs and other NPs. We
82 here investigated whether regression analysis could be used to assign absolute units of fluorescence
83 to stained EVs that are far out of the range of these calibrator intensity levels. We evaluated the
84 performance of the different calibrator beads sets and their inter-platform variation on three
85 different flow cytometers capable of single EV analysis. Finally, we studied how the use of
86 different bead sets would affect the calibration of fluorescence signals from synthetic NPs and
87 biological fluorescently stained and antibody labeled EVs.
88

89 **Material and Methods**

90

91 **MESF calibration beads**

92 For calibration of the fluorescence axis in the fluorescein isothiocyanate (FITC) channel we used
93 two different sets of FITC MESF beads (custom-made, 6 µm lot MM2307 #131-10; #131-8; #130-
94 6; #130-5 and 2 µm lot MM2307#156; #159.1; #159.2; #122.3, BD Biosciences, San Jose, CA).

95 For calibration of the fluorescence axis in the PE channel, we used two different sets of PE MESF
96 beads (6 µm, commercial QuantiBrite, Catalog. No. 340495 lot 62981 and 2 µm, custom made, lot
97 MM2327#153.1; #153.2; #153.4; #153.5; #153.6, BD Biosciences, San Jose, CA).
98 The 6 µm FITC MESF beads were prepared by reacting various concentration of FITC with PMMA
99 Beads (Bangs Labs) in borate buffer at pH 9.2. The 2 µm FITC beads were prepared by reacting
100 various concentrations of FITC-BSA (with a FITC/BSA molar ratio of 2) with 2 µm carboxylic
101 beads (Bangs Labs) using EDC/NHS chemistry. The 2 µm PE beads were made as described above
102 except various concentrations of PE were used with 2 µm carboxylic beads in EDC/NHS chemistry.
103 The beads were analyzed on LSR Fortessa™ (BD Biosciences) and their MESF values were
104 assigned using commercially available MESF beads (Flow Cytometry Standards Corp.) as
105 calibrators. The FITC ERF values were assigned to both 2 µm and 6 µm beads using a specific lot
106 of FITC-FC Bead (BD Biosciences) as a calibrator with known ERF value, which has been
107 assigned by NIST.
108
109 **Flow cytometer platforms**
110 In this study three flow cytometers were used. A jet in air-based BD Influx (BD Biosciences, San
111 Jose, CA), a BC CytoFLEX LX (Beckman Coulter, Brea, CA) with a cuvette-based system and a
112 cuvette-based SORP BD FACSCelesta™ (BD Biosciences, San Jose, CA) equipped with a small
113 particle side scatter (SSC) module.
114 The BD Influx flow cytometer was modified and optimized for detection of submicron-sized
115 particles [7]. In brief, FITC was excited with a 488 nm laser (Sapphire, Coherent 200 mW) and
116 fluorescence was collected through a 530/40 bandpass filter. PE was excited with a 562 nm laser
117 (Jive, Cobolt 150 mW) and fluorescence was collected through a 585/42 bandpass filter. Optical
118 configuration of the forward scatter detector was adapted by mounting a smaller pinhole and an

119 enlarged obscuration bar in order to reduce optical background. This reduced wide-angle FSC
120 (rwFSC) allowed detection of sub-micron particles above the background based on forward scatter
121 [7, 8].
122 Upon acquisition, all scatter and fluorescence parameters were set to a logarithmic scale. To
123 minimize day to day variations, the BD Influx was standardized at the beginning of each
124 experiment by running 100 and 200 nm yellow-green (505/515) FluoSphere beads (Invitrogen,
125 F8803 and F8848). The instrument was aligned until predefined MFI and scatter intensities where
126 reached with the smallest possible coefficient of variation (CV) for rw-FSC, SSC and fluorescence.
127 After optimal alignment, PMT settings required no or minimal day to day adjustment and ensured
128 that each measurement was comparable. MESF beads and NPs were measured with a FSC
129 threshold set at 1.0 while for biological EVs a fluorescence threshold was set at 0.67 by allowing
130 an event rate of 10-20 events/second while acquiring a clean PBS sample.
131 When performing quantitative and qualitative analysis of synthetic NP and biological EV samples,
132 preparations were diluted in PBS as indicated. Upon loading on the Influx, the sample was boosted
133 into the flow cytometer until events appeared, after which the system was allowed to stabilize for
134 30 seconds. Measurements were performed by a fixed 30 seconds time or by setting a gate around
135 the spike-in beads and allowing to record a defined number of events in the gate (80 000 events)
136 using BD FACS Sortware 1.01.654 (BD Biosciences).
137 The CytoFLEX LX was used without any tailor-made modifications in the configuration. Before
138 measurements, the manufacturer recommended startup and QC procedure were run first. All scatter
139 and fluorescence parameters were set to a logarithmic scale. FITC was measured with a 50 mW
140 488 nm laser and fluorescence was measured through a 525/40 band pass filter at gain 1.0. FITC
141 MESF beads were recorded with a FSC threshold at 1000. Measurements were performed using
142 CytExpert 2.1 (Beckman Coulter).

143 The SORP BD FACSCelesta™ was equipped with a small particle SSC module for improved
144 scatter detection. Before measurement, the standard setup and QC procedures were performed and
145 the recommended CS&T performance check was run to monitor performance on a daily basis and
146 to optimize laser delay. All scatter and fluorescence parameters were set to a logarithmic scale. 100
147 nm yellow-green (505/515) FluoSphere beads (Invitrogen, F8803) were acquired and used to set
148 optimal small particle-SSC and fluorescence (FITC detector) PMT-V values. FITC was measured
149 with a 100 mW 488 nm laser through a 530/30 band pass filter. FITC MESF beads were recorded
150 with a SSC threshold at 200. Measurements were performed using BD FACSDiva™ Software
151 v8.0.3 (BD Biosciences).
152 Further descriptions of each instrument and methods are provided in Data S1 (MIFlowCyt
153 checklist) and Data S2 (MiFlowCyt-EV framework).
154
155 **Preparation of FITC-doped silica nanoparticles**
156 Synthetic silica nanoparticles (SiNPs) of 550 nm diameter with six different FITC fluorescence
157 intensities were produced by using a modified method of literature reports [9-12]. Briefly, the
158 amine reactive FITC molecules were covalently linked to the silane coupling agent, (3-
159 aminopropyl)-triethoxylsilane (APTES) in anhydrous ethanol. Monodisperse silica seeds of ~90
160 nm prepared by using amino acid as the base catalyst [9, 10] were suspended in a solvent mixture
161 containing ethanol, water and ammonia. Then tetraethyl orthosilicate (TEOS) and different
162 volumes of APTES−FITC solutions were added for growing FITC-doped SiNPs by a modified
163 Stöber method [11, 12]. Upon washing three times with anhydrous ethanol, the FITC-doped SiNPs
164 were reacted with TEOS in the solvent mixture to allow growth of a silica layer. The synthesized
165 SiNPs were washed three times with anhydrous ethanol and stocked in anhydrous ethanol. The
166 diameters of SiNPs were measured by transmission electron microscopy.

167 **Isolation and fluorescent staining of biological Extracellular Vesicles for flow cytometric**
168 **analysis**

169 EV-containing samples were obtained from 4T1 mouse mammary carcinoma cell culture
170 supernatants (ATCC, Manassas, VA) as previously described [8, 13, 14]. EVs were stained with
171 5-(and-6)-Carboxyfluorescein diacetate succinimidyl ester (CFDA-SE, hereinafter referred as
172 CFSE) (ThermoFisher, catalog number C1157) and separated as described previously [7]. Briefly,
173 2 µl of the isolated 4T1 EVs (corresponding to a concentration of 1.44 E12 particles/mL as
174 determined by nanoparticle tracking analysis) were mixed with 18 µl PBS/0.1% aggregate-depleted
175 (ad)BSA. For antibody labeling, samples were first resuspended in 15.5 µL PBS/0.1% adBSA and
176 incubated with 0.5 µg of rat anti-mouse CD9-PE (Clone: KMC8, IgG2a, κ, lot 7268877, BD
177 Biosciences) or matched isotype antibodies (Rat IgG2a, κ, PE-conjugated, lot 8096525, BD
178 Biosciences) for 1h at RT while protected from light. EVs were then stained with 40 µM CFSE in
179 a final volume of 40 µl. The sealed tube was incubated for 2h at 37°C while protected from light.
180 Next, staining was stopped by adding 260 µl PBS/0.1% adBSA. After fluorescent staining, EVs
181 were separated from protein aggregates and free reagents by bottom-up density gradient
182 centrifugation in sucrose for 17.30 h at 192,000 g and 4°C using a SW40 rotor (k-factor 144.5;
183 Beckman Coulter, Fullerton, California, USA). Twelve fractions of 1 mL were then collected from
184 the top of the gradient and respective densities were determined by refractometry using an Atago
185 Illuminator (Japan). For analysis by flow cytometry, EV samples corresponding to a 1.14 g/mL
186 density were diluted 1:20 in PBS prior measurement. MIFlowCyt-EV guidelines [2] were followed
187 whenever applicable (Data S2).

188

189 **Concentration determination by using spike-in beads**

190 EV concentration was normalized using a spiked-in external standard containing 200 nm orange
191 (540/560) fluorescent beads (Invitrogen, F8809). The concentration of the beads was determined
192 by Flow NanoAnalyzer N30 (NanoFCM, Xiamen, China) and stocked at 5.7E10 particles/mL.
193 Beads were diluted 1:$10^4$ in PBS and added to the EV samples, mixed and measured on the flow
194 cytometer. Bead count was used to calculate the EV concentration.
195

196 **Data analysis**

197 For fluorescence calibration each bead peak population was gated using FlowJo Version 10.5.0
198 and MFI were obtained for further least square linear regression analysis. Data was handled in
199 Microsoft Excel and figures were prepared using GraphPad Prism version 8.0 (GraphPad Software
200 Inc). The software FCMPASS Version v2.17 was used to generate files with calibrated axis units
201 in the histograms and dot plots shown [15] (Software is available on
202 http://go.cancer.gov/a/y4ZeFtA).
203

204 **Data availability**

205 All EV data of our experiments have been submitted to the EV-TRACK knowledgebase (EV-
206 TRACK ID: EV210047)[16]. All flow cytometric data files have been deposited at the Flow
207 Repository (FR-FCM-Z3FJ).
208

209 **Results**

210 **Cross-platform assessment of MESF-bead based calibration of fluorescent signals using**
211 **different bead sets**

212 Two differently-sized FITC MESF bead sets of 6 µm and 2 µm, each containing 4 bead populations
213 per set and respectively representing an overall brighter (6 µm) and an overall dimmer (2 µm)

214 beads set, were measured and their use for fluorescence calibration of FITC fluorescent signals was
215 evaluated using three different flow cytometer platforms, namely a BD Influx, a BC CytoFLEX
216 and a SORP BD FACSCelesta. Every bead population measured on each of these three platforms
217 was gated and respective singlet gated populations are displayed as overlays in histograms (Figure
218 1a) showing their FITC fluorescence. The 4 peaks in the histograms of both the 6 µm and 2 µm
219 beads are indicated from dim to bright fluorescent as p1, p2, p3 and p4 (Figure 1b). The bigger
220 sized 6 µm FITC MESF beads contained overall brighter fluorescent intensities, whose assigned
221 values range from 25,910 to 715,225 FITC MESF. The smaller sized 2 µm FITC MESF beads
222 covered a dimmer part of the fluorescence intensity range with assigned values ranging from 3,634
223 to 103,706 FITC MESF. As expected, Figure 1b shows that MFI values alone expressed in arbitrary
224 units do not allow the comparison of measurements across the three instruments.
225 Therefore the FITC MFI of every bead population was next correlated to the FITC MESF values
226 provided for each bead population using least square linear regression. We found a different slope
227 in the two lines generated by either the 6 µm or the 2 µm MESF beads, consistent within each
228 platform and indicating that this is an inherent quality of these specific bead sets (Figure 1c). To
229 evaluate the precision and accuracy of FITC MESF assignments we used specific bead populations
230 from one set, referred to as 'unknown' in Figure 1, to calculate the FITC MESF by extrapolation
231 of the regression line based on the other bead set. The 'unknown' samples used where: 1) p1 and
232 p4 of the 2 µm bead set for which the FITC MESF values were calculated using the regression line
233 of the 6 µm bead set and 2) p1 and p2 of the 6 µm bead set for which the FITC MESF values were
234 calculated using the regression line of the 2 µm bead set (Figure 1c). Using this approach, the
235 extrapolated FITC MESF values of the 'unknown' p4 from the 2 µm beads and the 'unknown' p2
236 from the 6 µm beads could successfully be compared between platforms, proving the precision of

237 the fluorescence calibration and facilitating the interpretation of data acquired on the three different
238 platforms (Figure 1d-e and Figure 1h).
239 To quantify accuracy we decided to set a range of 20% difference as acceptable (10% above or
240 10% below actual values, as indicated by the green band in Figure 1d-e) for proper assignment to
241 MESF values. We found less than 20% difference from the expected value for all calculated FITC
242 MESF values of the 'unknown' signal from the p4 of the 2 µm beads on the 6 µm bead-set
243 regression line and the p2 of the 6 µm beads on the 2 µm bead-set regression line. This observation
244 was consistent for all platforms and independent of the bead set that was used. Thus, further
245 demonstrating not only precision but also the accuracy of fluorescence calibration (Figure 1d-e and
246 Figure 1h).
247 However, when extrapolating the 'unknown' bead signal from p1 of the 2 µm beads on the 6 µm
248 bead-set regression line and from p1 of the 6 µm beads on the 2 µm bead-set regression line (Figure
249 1f-g) we found that although calculated FITC MESF values were again comparable between
250 platforms and hence calibration proved to be precise, the accuracy was uncertain. Comparison of
251 the calculated MESF values of the 'unknown' beads to the expected MESF values in these cases
252 revealed more than a 20% difference, leading to either an underestimation or an overestimation of
253 the absolute number of FITC MESF (Figure 1f-h).
254 This can be explained by the fact that slight differences in the slope of the calibration lines of the
255 different bead sets become more prominent when the extrapolation is extended into the dimmer or
256 brighter range of the fluorescence intensities of the calibration beads, so out of the range of the
257 calibrators. Importantly, the same trend was observed in all three platforms evaluated. It is unlikely
258 that differences in slopes are caused by instrument non-linearity since it is a recurrent pattern on
259 all three platforms (Figure 1) and linear plotted values do not show non-linearity either (Figure
260 S1a-c). Also, variability between separate measurements could be excluded (Figure S2). Finally,

261 the same phenomenon occurred when 6 µm and 2 µm calibrator bead sets for PE MESF were used.
262 In this case the opposite situation occurred; the dimmer 2 µm beads displayed a steeper slope than
263 the brighter 6 µm beads (Figure S1d-f). Hence, our observations are pointing towards an
264 uncertainty in the assignment of the both FITC and PE beads.

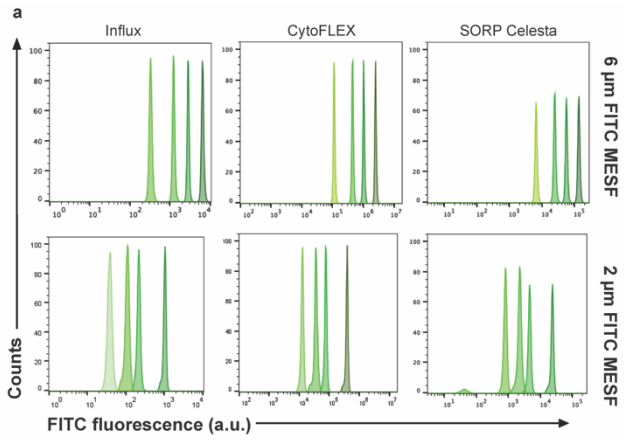


b

| | MFI | | | |
|---|---|---|---|---|
| 6 µm beads | Influx | CytoFLEX | SORP Celesta | FITC MESF |
| p1 | 317 | 107336 | 6321 | 25910 |
| p2 | 1173 | 421852 | 23322 | 118192 |
| p3 | 2684 | 962928 | 53219 | 275288 |
| p4 | 6111 | 2324148 | 127668 | 715225 |

Brightness

| | MFI | | | |
|---|---|---|---|---|
| 2 µm beads | Influx | CytoFLEX | SORP Celesta | FITC MESF |
| p1 | 37 | 12357 | 780 | 3634 |
| p2 | 106 | 34544 | 2169 | 10520 |
| p3 | 210 | 73054 | 4380 | 22841 |
| p4 | 991 | 367458 | 22370 | 103706 |

Brightness

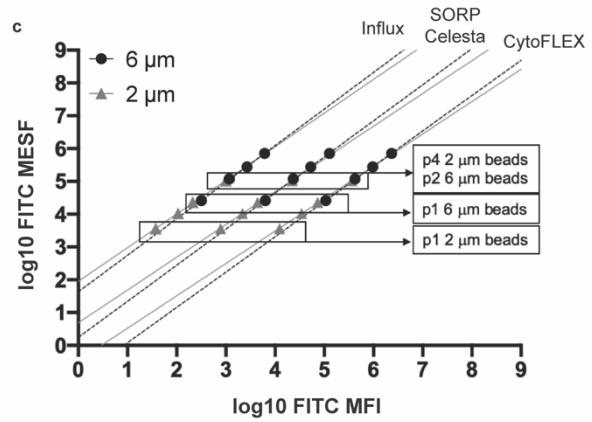


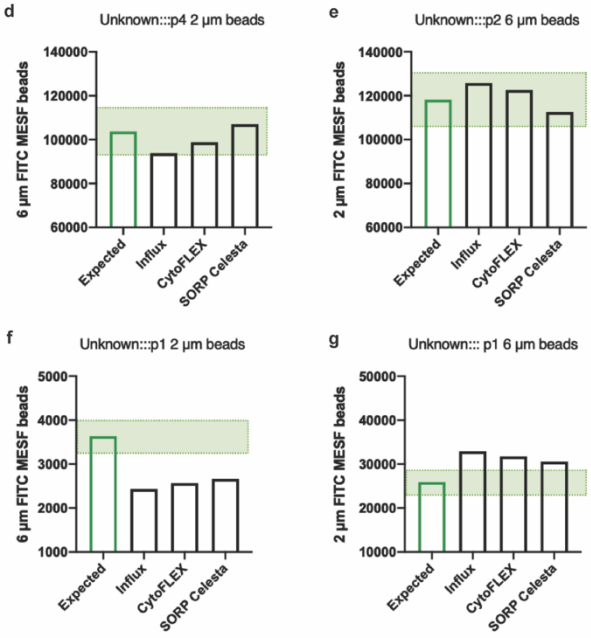


| | 6 µm FITC MESF beads | 2 µm FITC MESF beads |
|---|---|---|
| Influx | Y = 1.1146*X + 1.6325<br>$R^2$ = 0.9995 | Y = 1.0261*X + 1.951<br>$R^2$ = 0.9993 |
| CytoFLEX | Y = 1.0762*X – 0.9947<br>$R^2$ = 0.9998 | Y = 0.9869*X – 0.4632<br>$R^2$ = 0.9992 |
| SORP Celesta | Y = 1.1004*X – 0.2432<br>$R^2$ = 0.9993 | Y = 0.9989*X + 0.6884<br>$R^2$ = 0.9985 |

h

| | | Assigned FITC MESF | Calculated FITC MESF values | | |
|---|---|---|---|---|---|
| Used as calibrator | Used as unknown | Expected values | Influx | CytoFLEX | SORP Celesta |
| 6 µm FITC beads | p4:::2 µm FITC beads | 103706 | 93745 | 98759 | 107046 |
| 2 µm FITC beads | p2:::6 µm FITC beads | 118192 | 125680 | 122538 | 112554 |
| 6 µm FITC beads | p1:::2 µm FITC beads | 3634 | 2432 | 2565 | 2665 |
| 2 µm FITC beads | p1:::6 µm FITC beads | 25910 | 32904 | 31743 | 30550 |

265

266 **Figure 1. Evaluation of two different FITC MESF bead sets for the calibration of fluorescent**
267 **intensities across three flow cytometer platforms. (a)** Histogram overlays (axis in arbitrary units) of FITC
268 fluorescent intensity peaks derived from the 6 µm or the 2 µm FITC MESF beads **(b)** Table showing the
269 median fluorescence intensity (MFI) statistic derived from each of the fluorescent intensity peaks from
270 dimmer to brighter being expressed in arbitrary units. **(c)** Least square linear regression analysis of 6 µm
271 (black circles) and 2 µm (grey triangles) FITC MESF beads. Provided FITC MESF and measured FITC
272 MFI values were transformed to log and plotted in a log-log fashion for the three platforms. **(d-g)** Bar graphs
273 showing the expected absolute FITC MESF and the calculated FITC MESF values for different unknowns
274 as indicated in the figure. The absolute number of FITC MESF was calculated for the indicated fluorescent
275 intensity peak population and compared to the expected value on the three flow cytometers. For comparison,
276 we included a 20% variation from the expected FITC MESF of the population as a reference point (green).
277 **(h)** Table indicating the expected and calculated FITC MESF values for each sample used in the analysis.
278

279 **MESF assignments of FITC fluorescence intensities from synthetic silica nanoparticles**
280 **depend on the MESF-bead calibrator set used**

281 So far we have demonstrated that accuracy of assignment is negatively influenced when signal
282 strength of the unknown particle is further away from the average fluorescence intensities of the
283 calibrator beads. We next investigated how calibration with the FITC MESF bead-sets impact
284 absolute fluorescent assignment when nanoparticles with even dimmer fluorescence were
285 measured. For this purpose we selected one platform (BD Influx) to measure and analyze 550 nm
286 silica NPs, containing 6 populations with different FITC fluorescence intensities. Singlets were
287 gated (Figure S3) and an overlay histogram showing their 6 different FITC fluorescence intensities
288 was generated (Figure 2a, left). We next performed fluorescence calibration and generated two
289 additional histograms showing calibrated FITC MESF units based on either the 6 µm (Figure 2a,
290 middle) or the 2 µm FITC MESF calibrator bead set (Figure 2a, right). We obtained the MFI and

291 CV values for each population and further calculated their FITC MESF values based on the two
292 different FITC MESF calibrator bead sets (Figure 2b). Our data show that when using brighter 6
293 µm calibration beads, the calculated FITC MESF values were always lower as compared to the use
294 of the 2 µm bead-set regression line (Figure 2b). In addition, the multi-intensity peak analysis of
295 the silica NPs in one measurement revealed that the difference in the absolute FITC MESF values
296 of the synthetic silica NPs obtained by the two calibrator bead sets increased in the dimmer range
297 of the fluorescence, with a 27.3% variation for the highest fluorescent peak (p6) and 76.5%
298 variation for the dimmest population of these NPs (Figure 2b). To further visualize this, we used
299 the calculated FITC MESF values (Figure 2b) to generate an overlay bar graph showing the
300 differences in calculated FITC MESF from the six FITC fluorescent populations within the 550 nm
301 NPs (Figure 2c). Our results demonstrate that the variation between using the 6 µm (dark green) or
302 2 µm (light green) FITC MESF bead set progressively increased from brightest (p6) to dimmest
303 (p1) NP populations (Figure 2c). As indicated before, this can be ascribed to the differences in the
304 slopes of the regression lines of the two different bead sets and the extrapolation into the dim area.
305 To confirm that this phenomenon was not limited to the use of FITC MESF beads we additionally
306 analysed 6 µm and 2 µm PE MESF calibrator bead sets on the BD Influx (Figure S1d-f). By
307 measuring a sample containing 200 nm broad spectrum fluorescent polystyrene NPs we could
308 determine its fluorescent intensity in terms of ERF (Figure S4a). The variation in the absolute PE
309 ERF value obtained by the two different calibrator sets used to assign the absolute calibrated ERF
310 value was in this case 41.3% (Figure S4b).
311

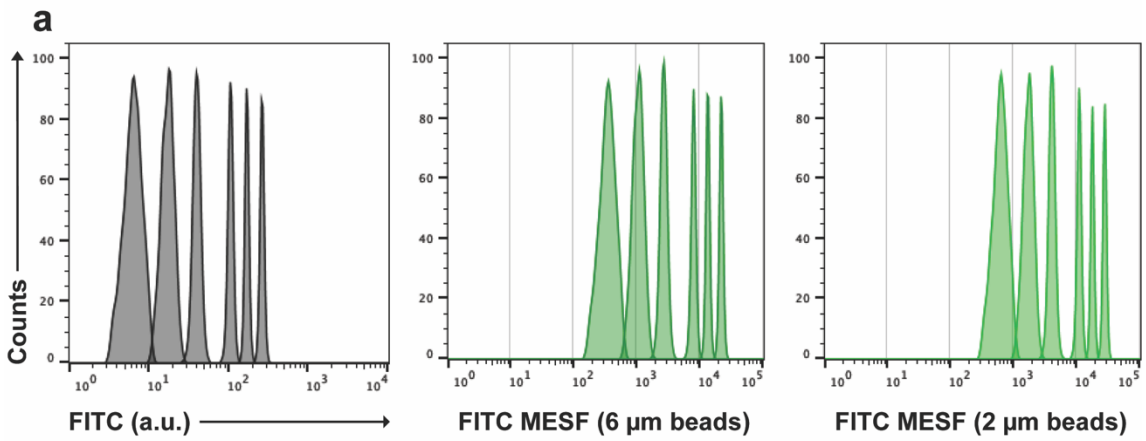


b

| | | | Calculated FITC MESF values Used as calibrator | | |
|---|---|---|---|---|---|
| Unknown | MFI | CV | 6 µm FITC beads | 2 µm FITC beads | % variation |
| p1 | 6.35 | 25.53 | 337 | 595 | 76.5 |
| p2 | 17.20 | 17.83 | 1022 | 1654 | 61.8 |
| p3 | 39.60 | 10.89 | 2590 | 3894 | 50.3 |
| p4 | 104.90 | 6.86 | 7671 | 10581 | 37.9 |
| p5 | 167.00 | 5.12 | 12881 | 17050 | 32.4 |
| p6 | 258.90 | 5.10 | 20995 | 26734 | 27.3 |

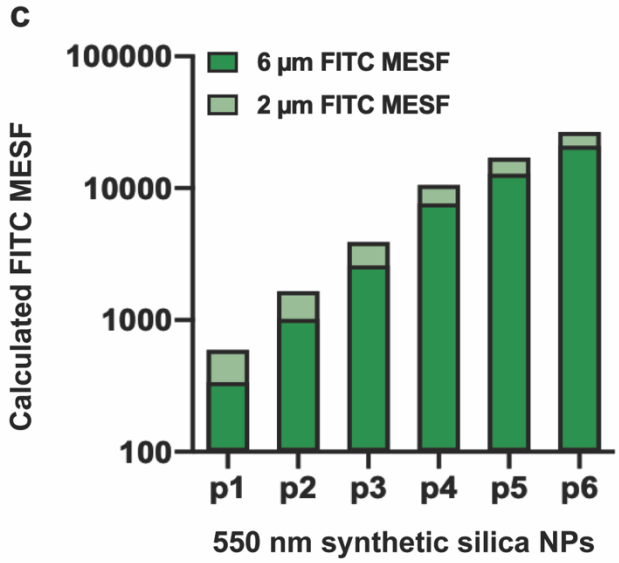


**Figure 2. MESF bead-based calibration of fluorescence signals from synthetic silica NPs. (a)** Histogram overlay showing FITC fluorescence in arbitrary units (a.u.) from each population next to FITC

315 MESF calibrated axis based on the 6 µm or 2 µm FITC MESF beads from the six differently FITC-labeled
316 550 nm NP gated populations. **(b)** Table showing the MFI and CV of each population and the calculated
317 FITC MESF values for each of the unknown populations with the percentage of variation between the two
318 calculated reference values. **(c)** Bar graph showing the calibrated FITC MESF values for each of the six
319 differently FITC-labeled populations based on the 6 µm (dark green, generally lower numbers) and 2 µm
320 (light green, generally higher numbers). Bars from 6 µm bead values and bars from 2 µm bead values are
321 presented as overlays.
322

323 **Different MESF-bead sets assign different absolute numbers of ERF and MESF to**
324 **fluorescently CFSE stained and CD9 labeled extracellular vesicles**

325 Next, we investigated the impact of this phenomenon on the assignment of absolute FITC-ERF
326 units and PE MESF units to a biological EV sample measured on the same platform by using the
327 four different calibration bead sets, i.e. 6 and 2 µm FITC MESF and the 6 and 2 µm PE MESF
328 beads. Since EVs scatter less light than beads and NPs, we used a fluorescence threshold to measure
329 the biological EVs [7]. To this end, we used CFSE as a luminal dye to fluorescently stain EVs and
330 a tetraspanin CD9 antibody, since this tetraspanin transmembrane protein is known to be enriched
331 in the surface of EVs and is considered as EV-marker. Next to the CFSE stained and CD9-PE
332 labeled EVs, we measured an unstained control containing EVs but without CFSE or antibody and
333 a matching isotype control (Figure 3a). Since 200 nm spike-in beads were added to the samples for
334 EV concentration measurement we defined an EV-gate and a spike-in bead gate in these samples
335 and relevant additional controls (Figure S5a). Our data revealed a 76.6% variation in the MFI
336 expressed in absolute CFSE ERF units on CFSE stained EV and a 156.9% variation in the MFI
337 expressed in absolute PE MESF units on CD9-PE labeled EVs when the two different calibrator
338 bead sets were used on the same platform (Figure 3a-b). The fluorescent threshold value of 0.67

339 used on the BD Influx corresponds to an equivalent of 150 FITC MESF based on the 6 µm beads
340 or 300 FITC MESF based on the 2 µm beads (Figure 3a) and indicates the level of detection using
341 this fluorescence threshold. Therefore, especially when a fluorescence threshold is used to measure
342 EVs, accurate calibrators are required to be able to report the fluorescence threshold in calibrated
343 units.
344 Lastly, in the overlay histograms it is shown how the fluorescence intensities of the calibrators
345 relate to the dimmer signals generated by CFSE stained and CD9-PE labeled EVs (Figure 3c-d).

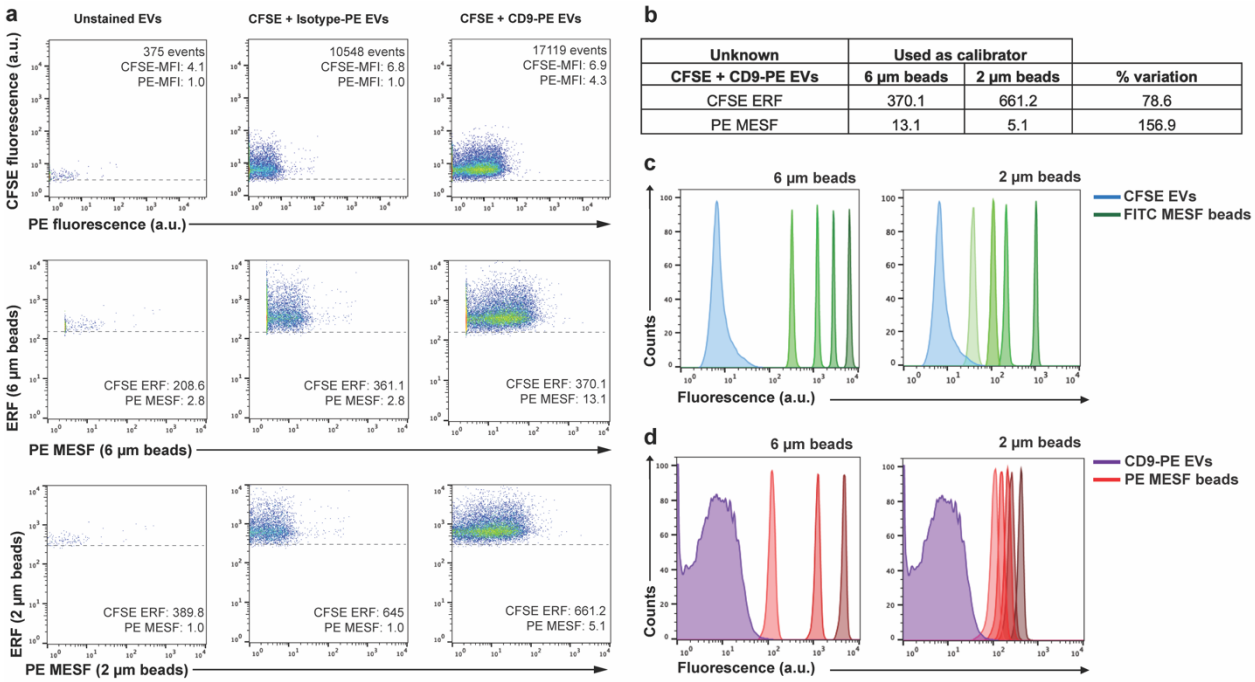


| Unknown | Used as calibrator | | |
|---|---|---|---|
| CFSE + CD9-PE EVs | 6 µm beads | 2 µm beads | % variation |
| CFSE ERF | 370.1 | 661.2 | 78.6 |
| PE MESF | 13.1 | 5.1 | 156.9 |

346

347 **Figure 3. MESF bead-based calibration of fluorescence signals from biological EV samples. (a)**
348 Analysis of three biological EV samples by using a fluorescence threshold. Unstained EVs control, CFSE
349 + isotype-PE EVs next to CFSE + CD9-PE stained EVs (from left to right plots) with dot plots showing
350 CFSE fluorescence vs PE fluorescence in arbitrary units (a.u.) (upper row) or CFSE ERF vs PE MESF
351 calibrated axis based on either the 6 µm (middle row) or 2 µm beads (lower row). The discontinuous line in
352 each dot plot indicates the fluorescence threshold value used, which is 0.67 and on this BD Influx
353 corresponds to an equivalent of 150 FITC MESF based on the 6 µm beads or 300 FITC MESF based on the

354 2 µm beads. Number of events for each sample within the EV gate and MFI values for either CFSE or PE
355 fluorescence (a.u.) are indicated in the top row. Once calibrated dot plots were generated the median
356 fluorescence intensity in either CFSE ERF or PE MESF standardized units of fluorescence were obtained
357 based on the 6 µm (middle row) or 2 µm beads (lower row) and are indicated for each dot plot. **(b)** Table
358 showing the ERF or MESF values obtained after calibration for the CFSE + CD9-PE EVs and the percentage
359 of variation between the use of the 6 µm or 2 µm bead sets. **(c)** Histogram overlays displaying fluorescence
360 in arbitrary units from CFSE stained EVs (blue) next to the 6 µm or 2 µm FITC MESF bead set (green). **(d)**
361 Histogram overlays displaying fluorescence in arbitrary units from CD9-PE labeled EVs (purple) next to
362 the 6 µm or 2 µm PE MESF bead set (red).
363

364 **Discussion**

365 The calibration of fluorescence measurements obtained by flow cytometry in terms of MESF or
366 ERF is essential for proper and robust comparison of data between different instruments, different
367 labs and different time points. EV flow cytometry is pursued as a tool in the rapidly expanding EV
368 research field and the definition of what and how much can be detected is only starting to evolve.
369 Besides the inter-comparability of EV data, the use of calibrated values also allows to create
370 consensus about the range of fluorescence that can be expected by EV flow cytometry in case of
371 generic staining and epitope density, thereby facilitating the further identification of EV in flow
372 cytometry data. Therefore, it is desirable to express flow cytometry data from EVs in calibrated
373 units as well [2]. Our results clearly illustrate why it is important to perform fluorescence
374 calibration, as previously reported in other studies [17, 18], since MFI values in arbitrary units
375 cannot be directly compared when samples are measured on different flow cytometers.

376 Our findings show that extrapolating bright reference beads to dim signals is possible and calibrated
377 values are precise irrespective the instrument used, allowing standard comparisons, which is in line

378 with earlier findings [18]. However, the accuracy of assigning absolute MESF or ERF values relies
379 for a great deal on the exactness by which the calibrator beads are assigned. The effect of small
380 variations in assignment may cause uncertainty in the slopes of the regression lines. The uncertainty
381 in the slope affects the uncertainty for a particular point based on the spread of the points. Since
382 the points at the ends (low intensity end) are farthest away, the uncertainty increases with the
383 distance to the other points on average [19]. On the other hand, difference in slope between two
384 calibrator sets per definition denotes an interception point somewhere along the line. Comparability
385 may fully depend on the position of the interception point. In our study the interception point is
386 close to the range where the beads reside and goes hand in hand with precision and accuracy for
387 values in this range. However away from this point, larger uncertainties occur due to the further
388 separation of the two regression lines. The currently available commercial MESF beads are
389 designed to calibrate fluorescence intensity in the range of regular cell flow cytometry. However,
390 EVs are orders of magnitude smaller than cells and their fluorescence based on generic staining or
391 based on antibody labeling and epitope density is far dimmer than the available calibrators. To
392 assign numbers of fluorophores to these weak signals, we rely on extrapolation of the regression
393 line into the dim area. In this proof-of-principle study, we show that the intrinsic uncertainty of the
394 number of assigned fluorescent molecules per calibrator bead induces a higher deviation from the
395 expected value of MESF when the regression line is followed into the area of the dimmer particles.

396 It may be clear from our results with the unknown synthetic NPs and the biological EVs that the
397 outcome of the results definitively depends on the calibrator used. Since calibration is an essential
398 part in the identification and inter-comparability of EV data, we therefore advise that proper
399 reporting of how fluorescent calibration is being done and adequate description of materials needs
400 to be included to avoid confusing interpretation of calibrated data. Hence, we propose that not only

401 absolute fluorescence values need to be reported but also the calibration bead set and lot number
402 used, including all MFI and MESF values. Furthermore, for future benchmarking and comparison
403 studies, ideally the same calibrator sets should be used. Clearly, a calibrator that has a low
404 uncertainty of assignment and has MESF values closer to the range of fluorescence intensity of the
405 unknown particle of interest is most preferable and determination of absolute MESF/ERF values
406 to NPs and EVs needs to be further investigated and validated before robust conclusions can be
407 made. Moreover, novel state-of-the-art flow cytometers that are designed to measure small particles
408 rely obligately on sub-micron beads to perform MESF calibration. These state-of-the-art platforms
409 cannot measure the 'standard' 6 µm or 2 µm MESF beads [20]. Therefore, there is an urgent need
410 for small and dim calibration beads that are especially designed for NPs and EVs to be widely used
411 in cross-platform and inter-laboratory comparisons.
412 In summary, our results indicate that calibration of fluorescent signals is crucial for comparison
413 between platforms, and that it should be utilized and properly reported. Nevertheless, accurate
414 assignment of MESF/ERF to particles in the sub-micron size range could be hampered by the
415 inherent uncertainty of the calibrators. Therefore, statements on the absolute number of
416 fluorescence units, either MESF or ERF, present on NPs and EVs are related to the calibrator set
417 used. To avoid inconsistencies, so far calibration for inter-comparison may preferably be performed
418 using identical calibrator bead lots. For more robust assignments of fluorescence units to NPs and
419 EVs there is a need for calibration materials that have low uncertainty of assigned fluorescent
420 values and have a size range that is compatible for all flow cytometer platforms used for analysis
421 of sub-micron sized particles, including both NPs and EVs.
422
423 **Funding Statement**

This research is supported by the European Union's Horizon 2020 research and innovation programme under the Marie Skłodowska-Curie grant agreement No 722148 and by the National Natural Science Foundation of China (21934004 and 21627811). E.L.A. is supported by the European Union's Horizon 2020 research and innovation programme under the Marie Skłodowska-Curie grant agreement No 722148.

**Author Contributions**

E.L.A. designed and performed experiments, analyzed data and wrote the manuscript. T.B. performed experiments and gave conceptual advice. L.W. gave technical and conceptual advice. M.M., Y.T. and X.Y. prepared materials and gave technical advice. G.J.A.A. and M.H.M.W. supervised the research, designed (performed) experiments and wrote the manuscript. G.J.A.A. and M.H.M.W. contributed equally as senior author. All authors critically reviewed and edited the manuscript.

**Acknowledgments**

The authors would like to thank Prof. An Hendrix (Laboratory of Experimental Cancer Research, Ghent University, Belgium) for the possibility to prepare and analyze M4T1 derived EV in her lab, Dr. Joshua A. Welsh (National Cancer Institute, Bethesda, MD) for helpful discussion and Ludo Monheim (BD Biosciences, Erembodegem, Belgium) for helpful technical support. FITC MESF and 2 μm PE MESF beads were kindly provided by BD Biosciences (prepared by Dr. Majid Mehrpouyan) as part of the European Union's Horizon 2020 research and innovation programme under the Marie Skłodowska-Curie grant agreement No 722148.

**Declaration of interest disclosure**

Tina Van Den Broeck and Majid Mehrpouyan are both employees of BD Biosciences, a business unit of Becton, Dickinson and Company. During the course of this study, the Wauben research group, Utrecht University, Faculty of Veterinary Medicine, Department of Biomolecular Health Sciences and BD Biosciences collaborated as a co-joined partner in the European Union's Horizon 2020 research and innovation programme under the Marie Skłodowska-Curie grant agreement No 722148. Xiaomei Yan declares competing financial interests as a cofounder of NanoFCM Inc., a company committed to commercializing the nano-flow cytometry (nFCM) technology.

**Supporting Information**

Additional supporting information can be found online in the corresponding section at the end of the article.

**Data S1.** Author Checklist: MIFlowCyt-Compliant Items.

**Data S2.** MIFlowCyt-EV framework.

**Figure S1.** Analysis of different MESF bead sets measured on the BD Influx.

**Figure S2.** Evaluation of measurement variability of 2 µm FITC MESF beads measured on the BD Influx.

**Figure S3.** Gating strategy for synthetic silica NPs.

**Figure S4.** 200 nm fluorescent polystyrene NPs.

**Figure S5.** Gating strategy for external spiked-in beads and biological EV samples.

**ORCID**

Estefanía Lozano-Andrés https://orcid.org/0000-0002-7305-0776

Lili Wang https://orcid.org/0000-0003-2456-898X

Xiaomei Yan http://orcid.org/0000-0002-7482-6863

Marca H.M. Wauben https://orcid.org/0000-0003-0360-0311

Ger. J.A. Arkesteijn https://orcid.org/0000-0001-7739-582X

## References

1. Nolan, J.P., *Flow Cytometry of Extracellular Vesicles: Potential, Pitfalls, and Prospects.* Curr Protoc Cytom, 2015. **73**: p. 13 14 1-16.
2. Welsh, J.A., et al., *MIFlowCyt-EV: a framework for standardized reporting of extracellular vesicle flow cytometry experiments.* J Extracell Vesicles, 2020. **9**(1): p. 1713526.
3. Hoffman, R.A., *Standardization, calibration, and control in flow cytometry.* Curr Protoc Cytom, 2005. **Chapter 1**: p. Unit 1 3.
4. Wang, L. and R.A. Hoffman, *Standardization, Calibration, and Control in Flow Cytometry.* Curr Protoc Cytom, 2017. **79**: p. 1 3 1-1 3 27.
5. Gaigalas, A.K., et al., *Quantitating Fluorescence Intensity From Fluorophore: Assignment of MESF Values.* J Res Natl Inst Stand Technol, 2005. **110**(2): p. 101-14.
6. Wang, L., et al., *Quantitating Fluorescence Intensity From Fluorophores: Practical Use of MESF Values.* J Res Natl Inst Stand Technol, 2002. **107**(4): p. 339-53.
7. van der Vlist, E.J., et al., *Fluorescent labeling of nano-sized vesicles released by cells and subsequent quantitative and qualitative analysis by high-resolution flow cytometry.* Nat Protoc, 2012. **7**(7): p. 1311-26.
8. Arkesteijn, G.J.A., et al., *Improved Flow Cytometric Light Scatter Detection of Submicron-Sized Particles by Reduction of Optical Background Signals.* Cytometry A, 2020. **97**(6): p. 610-619.
9. Yokoi, T., et al., *Periodic arrangement of silica nanospheres assisted by amino acids.* J Am Chem Soc, 2006. **128**(42): p. 13664-5.
10. Yokoi, T., et al., *Mechanism of Formation of Uniform-Sized Silica Nanospheres Catalyzed by Basic Amino Acids.* Chemistry of Materials, 2009. **21**(15): p. 3719-3729.
11. Stöber, W., A. Fink, and E. Bohn, *Controlled growth of monodisperse silica spheres in the micron size range.* Journal of Colloid and Interface Science, 1968. **26**(1): p. 62-69.
12. Giesche, H., *Synthesis of monodispersed silica powders II. Controlled growth reaction and continuous production process.* Journal of the European Ceramic Society, 1994. **14**(3): p. 205-214.
13. Vergauwen, G., et al., *Confounding factors of ultrafiltration and protein analysis in extracellular vesicle research.* Sci Rep, 2017. **7**(1): p. 2704.
14. Geeurickx, E., et al., *The generation and use of recombinant extracellular vesicles as biological reference material.* Nat Commun, 2019. **10**(1): p. 3288.
15. Welsh, J.A., et al., *FCMPASS Software Aids Extracellular Vesicle Light Scatter Standardization.* Cytometry A, 2019.
16. Consortium, E.-T., et al., *EV-TRACK: transparent reporting and centralizing knowledge in extracellular vesicle research.* Nat Methods, 2017. **14**(3): p. 228-232.
17. Nolan, J.P. and S.A. Stoner, *A trigger channel threshold artifact in nanoparticle analysis.* Cytometry A, 2013. **83**(3): p. 301-5.
18. Welsh, J.A., J.C. Jones, and V.A. Tang, *Fluorescence and Light Scatter Calibration Allow Comparisons of Small Particle Data in Standard Units across Different Flow Cytometry Platforms and Detector Settings.* Cytometry A, 2020. **97**(6): p. 592-601.
19. Draper, N.R. and H. Smith, *Applied regression analysis*. 1981, New York: Wiley.
20. Tian, Y., et al., *Protein Profiling and Sizing of Extracellular Vesicles from Colorectal Cancer Patients via Flow Cytometry.* ACS Nano, 2018. **12**(1): p. 671-680.